

Original Article

Construction of the ceRNA network in the progression of acute myocardial infarction

Hui Liu*, Shuai Qin*, Yuanyuan Zhao, Lei Gao, Chao Zhang

Department of Cardiovascular Surgery, Linfen Central Hospital, Linfen, Shanxi, China. *Equal contributors.

Received August 17, 2022; Accepted November 11, 2022; Epub December 15, 2022; Published December 30, 2022

Abstract: Acute myocardial infarction (AMI) is a common disease that induced by sudden occlusion of a coronary artery and myocardial necrosis, which causes a great medical burden worldwide. Noncoding RNAs, such as circRNA, lncRNA and miRNA, play crucial roles in the progression of cardiovascular diseases. However, the circRNA-miRNA-mRNA network in the occurrence and development of AMI needs further investigation. In this study, we downloaded three AMI datasets, including circRNA (GSE160717), miRNA (GSE24591), and mRNA (GSE66360) from GEO database. The differentially expressed candidates, and GO and KEGG functions were analyzed by RStudio, and subsequently import to PPI and Cytoscape to obtain the hub genes. By using the starbase target prediction database, we further screen the ceRNA network of circRNA-miRNA-mRNA based on the selected differentially expressed candidates. We found 46 differential expressed mRNAs, 65 miRNAs, and five circRNAs. GO functions and KEGG enrichment of the 46 mRNAs focused on immune response and functions, involving IL-17 signaling pathway, Toll-like receptor signaling pathway, cytokine-cytokine receptor interaction, TNF signaling pathway, chemokine signaling pathway, and NF-kappaB signaling pathway, which may aggravate the pathologies of AMI. PPI and Cytoscape analysis showed 10 hub genes, including TLR2, IL1B, CCL4, CCL3, CCR5, TREM1, CXCL2, NLRP3, CSF3, and CCL20. By using starbase and circinteractome databases, ceRNA network construction showed that circRNA_023461 and circRNA_400027 regulate several miRNA-mRNA axes in AMI. In summary, this study uncovered the circRNA-miRNA-mRNA network based on three AMI datasets. The differentially expressed genes, including CCL20, CCL4, CSF3, and IL1B, focus on immune functions and pathways. Furthermore, circRNA_023461 and circRNA_400027 regulate several miRNA-mRNA axes, exerting important roles in AMI progression. Our founding provides new insights into AMI and improve the therapeutic strategies for AMI.

Keywords: ceRNA network, circRNA-miRNA-mRNA, acute myocardial infarction

Introduction

Acute myocardial infarction (AMI) is a common disease that induced by sudden occlusion of a coronary artery and myocardial necrosis [1]. The incidence of AMI is increasing year by year with a serious threat to human health and survival quality worldwide [2]. Early diagnosis and treatment are extremely important to improve the survival quality and prognosis of AMI patients. Up to date, biomarkers, including troponin I (TnI) and creatine kinase isoenzyme (CKMB) are applied for the diagnosis of AMI. Unfortunately, the treatment effect of AMI is still unsatisfactory since a poor understanding of its pathogenesis and underlying mechanisms [3, 4]. Therefore, the pathological mechanisms of AMI are urgently needed to be inves-

tigated and identifying new targets for the therapy or diagnosis of AMI are valuable.

Multiple of studies have suggested that non-coding RNAs, such as circular RNA (circRNA), long noncoding RNA (lncRNA) and microRNA (miRNA), play crucial roles in the progression of cardiovascular diseases [5]. miRNA is a type of endogenous small, single-stranded RNA molecule with about 18 to 24 nucleotides, which negatively modulates the downstream mRNA expression [6, 7]. CircRNA is spliced by exons at specific splicing sites to form a covalently closed continuous loop [8]. CircRNAs act as a competitive endogenous RNA (ceRNA) and sponge miRNA to regulate mRNA expression [9, 10]. Thus, the circRNA-miRNA-mRNA interaction exerts important roles in the occurrence

and development in cardiovascular diseases [11]. For instance, decreased miR-21-5p expression and upregulated circRNA_0031672 and PDCD4 expressions have been found in the patients with myocardial ischemia/reperfusion (IR) injury, miR-21-5p-expressing bone marrow mesenchymal stem cells alleviate myocardial IR injury by inhibiting the expression of circRNA_0031672 [11]. In addition, circRNA Cdy1 elevates abdominal aortic aneurysm formation by inducing M1 macrophage polarization and M1-type inflammation by repressing IRF4 entry into the nucleus [12]. Furthermore, circRNA USP36 promotes endothelial cell dysfunction in atherosclerosis by suppressing miR-637 to elevate the level of WNT4, upregulation of circRNA USP36 significantly represses proliferation and migration of ox-LDL-treated endothelial cells [13]. And CircRNA ACSL1 aggravated myocardial inflammation and myocardial injury by downregulating miR-8055 and enhancing the level of MAPK14. Silencing of circRNA ACSL1 or overexpression of miR-8055 significantly repressed myocardial inflammation and myocardial injury level, and overexpression of MAPK14 evidently rescues those effects [14].

Recent years, some studies revealed the role of circRNAs in myocardial infarction (MI) rat or mice models. Wang et al. demonstrated that circRNA MFACR is increased in MI and inhibits the expression of miR-125b, resulting in cardiomyocyte apoptosis induced by hypoxia in AC16 cells [15]. Liu et al. uncovered that circRNA ACAP2 promotes myocardial apoptosis by repressing the expression of miR-29 in MI rats [16]. Moreover, upregulation of circRNA SNRK significantly downregulates miR-103-3p to decrease cardiomyocyte apoptosis, promote cardiomyocyte proliferation, enhance angiogenesis, and improve cardiac functions through modulating GSK3 β / β -catenin pathway in MI rats [17]. Therefore, the ceRNA network plays important roles in the progression of MI. However, the circRNA-miRNA-mRNA network in the occurrence and development of AMI remains unclear. Notably, many studies analyze the public datasets based on microarray sequencing on human cardiovascular diseases tissues to construct the ceRNA networks. For instance, Mao et al. identified a serum exosomal-associated lncRNA/circRNA-miRNA-mRNA network in coronary heart disease based on the exoRBase database, and suggested RPL7AP11/hsa-miR-17-5p/UBC and RPL7AP11/hsa-miR-20b-5p/UBC axes may regulate

the pathogenesis of coronary heart disease [18]. Liu et al. constructed a ceRNA network associated with the development and prognosis of human atherosclerosis based on the GEO database. They constructed ceRNA network of the differentially expressed 9 lncRNAs, 29 miRNAs, and 90 mRNAs through three datasets [19].

In this study, we analyzed the circRNA-miRNA-mRNA network based on three datasets, including circRNA (GSE160717), miRNA (GSE24591), and mRNA (GSE66360). The differentially expressed candidates, and Gene Ontology (GO) and Kyoto Encyclopedia of Genes and Genomes (KEGG) functions were analyzed by RStudio, and subsequently imported to Cytoscape to obtain the hub genes. By using the target prediction database, we further screened the ceRNA network of the key circRNA-miRNA-mRNA in AMI tissues. Our findings may provide new insights into AMI and improve the diagnose and therapeutic strategies for AMI patients.

Methods

Microarray datasets

Microarray data of AMIs, with key words “acute myocardial infarction” and “Homo sapiens” filtration, were downloaded from the Gene Expression Omnibus (GEO, <https://www.ncbi.nlm.nih.gov/geo/>) database. Three datasets including circRNA, miRNA, and mRNA based on AMI patients and normal tissues were selected for further study. The data of the circRNA expression data (GSE160717) microarray platform was 074301 Arraystar Human CircRNA microarray V2 (platform: GPL21825) with six samples (three controls and three patients). The data of the miRNA expression data (GSE24591) microarray platform was Agilent-019118 Human miRNA Microarray 2.0 G44-70B (platform: GPL8227) with seven samples (three controls and four patients). The data of the mRNA expression data (GSE66360) microarray platform was Affymetrix Human Genome U133 Plus 2.0 Array (platform: GPL570) with 99 samples (50 controls and 49 patients).

Differential expression analysis

The volcano plots of differentially expressed circRNAs, miRNAs, and mRNAs were analyzed by the GEO2R online analysis tool. The differentially expressed genes (mRNA), differentially

expressed circRNAs (circRNA), and differentially expressed miRNAs (miRNA) analysis method for the datasets is the “Linear Models for Microarray Data (limma)” R package (version 3.26.8). The selection criteria set for adjusted P value < 0.05 . The AMI group was compared with the normal group, and the volcano plots were exported directly from the online analysis.

Functional enrichment and pathway analysis

The bar plots of Gene Ontology (GO) functions of the selected differentially expressed genes including biological process, cellular component, and molecular function, and the dot plot and bar plot of the Kyoto Encyclopedia of Genes and Genomes (KEGG) pathways of the selected differentially expressed genes were analyzed by the “clusterProfiler” R package (version 3.18.1).

Protein-protein interaction network analysis

The selected differentially expressed genes-encoded proteins were uploaded on the Search Tool for the Retrieval of Interacting Genes (STRING, <http://string-db.org>) online database to predict the PPI network. The interaction proteins list was downloaded and subsequently imported into Cytoscape (version 3.7.2) to visualize the PPI network based on Molecular Complex Detection (MCODE) algorithm. To explore the hub proteins in the list, cytoHubba algorithm was applied to search the hub genes. The differentially expressed genes with the 10 highest degree values were considered to be hub genes.

Prediction of target miRNAs for mRNA

The miRNA-mRNA interactions were predicted from the starbase database (<https://starbase.sysu.edu.cn/>), the targeting miRNAs of the 10 hub genes was obtained, and the Venn diagram was applied to obtain the same regulated pattern of the targeting miRNAs and the differentially expressed miRNAs of the GSE24591 from the online tool Venny (version 2.1.0) (<https://bioinfogp.cnb.csic.es/tools/venny/>).

CircRNA-miRNA-mRNA network construction

The targeting miRNAs of circRNA were predicted by the Circinteractome database (<https://circinteractome.nia.nih.gov/>). The ceRNA network was constructed based on the commonly

interactive differentially expressed miRNAs, differentially expressed hub genes, and differentially expressed circRNAs ($|\logFC$ (fold change) > 2 , and adjusted P value < 0.01). The circRNA-miRNA-mRNA ceRNA network was plotted from <http://www.bioinformatics.com.cn>, a free online platform for data analysis and visualization.

Results

Identification of differentially expressed circRNAs, miRNAs, and mRNAs

We first investigated the expression of differentially expressed circRNAs (GSE160717), miRNAs (GSE24591), and mRNAs (GSE66360) from the GEO datasets based on the GEO2R online analysis tool. The AMI group was compared with the normal group, and the volcano plots of the three datasets were exported directly from the online analysis on the criteria of adjusted P value < 0.05 (**Figure 1A-C**). Next, we selected the differentially expressed genes based on the thresholds including $|\logFC| > 2$, and adjusted P value < 0.01 . We found that 44 genes were upregulated and two genes were downregulated (**Table 1**). The top 10 most significantly upregulated genes in the AMI group sorted by \logFC were NR4A2, S100A12, ITLN1, CSTA, IL1B, TREM1, CCL20, FCER1G, PTX3, and IL1R2. And the only two downregulated genes were XIST and TSIX.

GO function and KEGG pathway enrichment analysis

The 46 differentially expressed genes were further applied to GO function and KEGG pathway enrichment analysis. The GO function annotation included biological process (BP), cellular components (CC), and molecular functions (MF). Regarding BP, neutrophil chemotaxis, neutrophil migration, granulocyte chemotaxis, granulocyte migration, neutrophil degranulation, myeloid leukocyte migration, neutrophil activation involved in immune response, and leukocyte chemotaxis processes were enriched, suggesting the immune functions play crucial roles in the development of AMI (**Figure 2A**). For CC, the results were centralized at tertiary granule, secretory granule membrane, secretory granule lumen, and cytoplasmic vesicle lumen (**Figure 2B**). And MF mainly focused on chemokine activity, immune receptor activity, chemokine receptor binding, and cytokine

ceRNA network in acute myocardial infarction

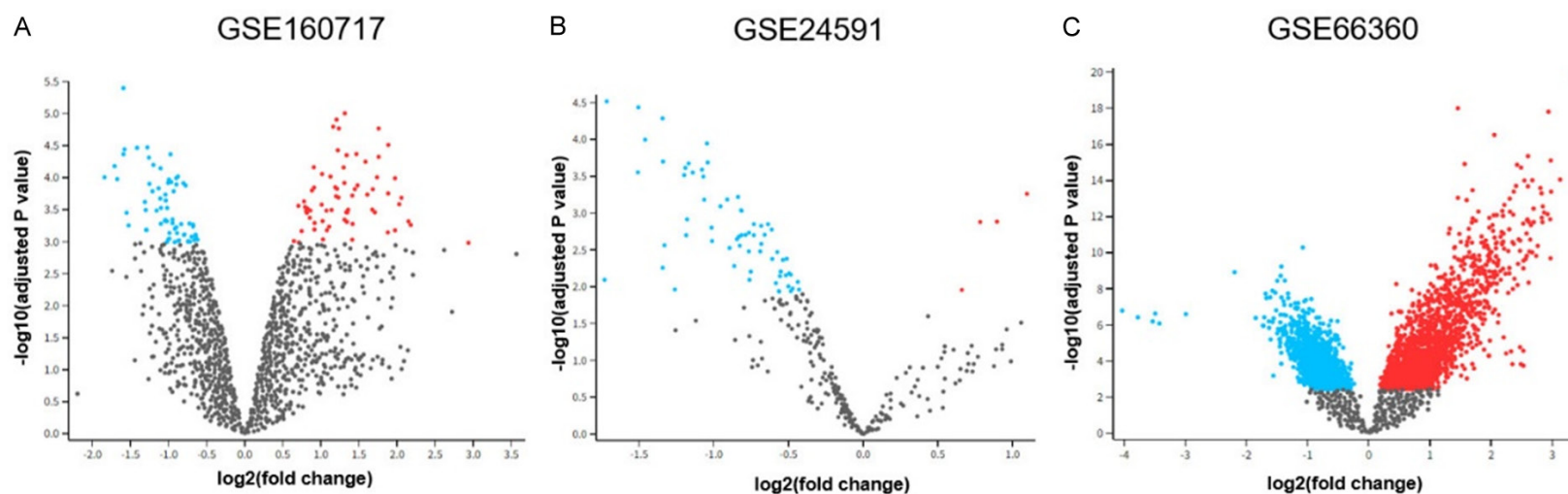


Figure 1. Volcano plots of differentially expressed candidates. A. GSE160717; circRNA; B. GSE24591; miRNA; C. GSE66360; mRNA. Blue spots: upregulated RNA molecules; red spots: downregulated RNA molecules. Differentially expressed RNA molecules were screened under the cut-off criteria adjusted *P* value ($P < 0.05$).

ceRNA network in acute myocardial infarction

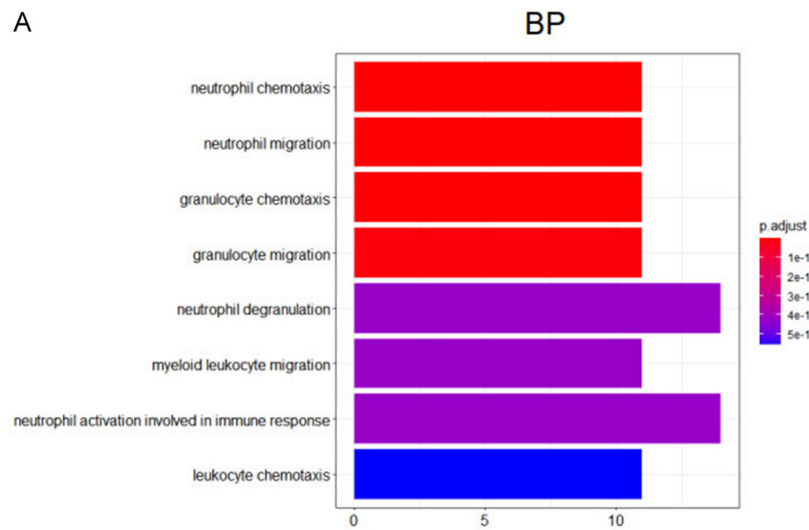
Table 1. The differentially expressed mRNAs in GSE66360 dataset

Gene	logFC	AveExpr	t	P.Value	adj.P.Val	B
NR4A2	2.997276	7.954906	11.63536	2.17E-20	5.11E-16	35.44236
S100A12	2.982203	7.879705	8.793435	3.91E-14	9.19E-11	21.66765
ITLN1	2.830404	6.738442	8.130369	1.09E-12	1.07E-09	18.46982
CSTA	2.76357	8.420818	7.401095	4.04E-11	1.64E-08	15.00874
IL1B	2.730999	9.225993	8.294584	4.81E-13	5.66E-10	19.25829
TREM1	2.697704	7.523257	8.01788	1.92E-12	1.56E-09	17.93136
CCL20	2.695502	8.510152	8.365843	3.37E-13	4.40E-10	19.60125
FCER1G	2.658921	8.587825	7.522325	2.23E-11	1.05E-08	15.57865
PTX3	2.614706	6.857152	6.4197	4.43E-09	7.90E-07	10.50573
IL1R2	2.607652	7.51075	9.314961	2.78E-15	8.35E-12	24.20144
CCL3	2.566784	9.301245	7.060749	2.11E-10	5.84E-08	13.42304
RPS4Y1	2.529927	9.813793	3.883932	0.000183	0.004466	0.432742
VCAN	2.516302	7.074636	7.94306	2.78E-12	2.18E-09	17.57403
CLEC4D	2.495079	6.075979	8.355111	3.55E-13	4.40E-10	19.54957
NFIL3	2.490702	8.614063	9.408688	1.73E-15	6.77E-12	24.65769
KDM5D	2.487632	8.117798	3.93849	0.000151	0.00383	0.61525
AQP9	2.472692	7.628128	7.273078	7.54E-11	2.69E-08	14.40971
IRAK3	2.378948	6.508487	9.950217	1.10E-16	6.47E-13	27.29498
C5AR1	2.297577	9.204937	6.819185	6.72E-10	1.61E-07	12.31206
S100P	2.296663	8.431091	7.835603	4.75E-12	3.38E-09	17.06205
NLRP3	2.234739	6.326847	8.606796	1.00E-13	1.70E-10	20.76408
LYZ	2.214456	9.168719	7.184194	1.16E-10	3.84E-08	13.99559
QPCT	2.203715	6.929869	7.724537	8.23E-12	5.23E-09	16.5345
CD83	2.181295	9.334758	7.450594	3.17E-11	1.35E-08	15.24114
CSF3R	2.174549	7.360479	7.060693	2.11E-10	5.84E-08	13.42278
TP53INP2	2.173989	7.976927	7.768411	6.62E-12	4.58E-09	16.74269
APOBEC3A	2.155174	7.731038	7.646806	1.21E-11	6.76E-09	16.16633
ACSL1	2.144376	8.276354	8.608759	9.92E-14	1.70E-10	20.77357
MAFB	2.135498	7.495932	8.172691	8.86E-13	9.41E-10	18.67276
CCL4	2.114274	9.132837	6.946528	3.65E-10	9.44E-08	12.89611
FCN1	2.094224	7.116857	7.497877	2.51E-11	1.14E-08	15.46352
LILRB2	2.090534	7.454025	7.927872	3.00E-12	2.28E-09	17.50158
PLBD1	2.085516	8.321705	6.182372	1.33E-08	2.06E-06	9.45343
BST1	2.079977	6.644763	7.469354	2.89E-11	1.28E-08	15.32933
S100A9	2.079914	9.307357	7.345251	5.30E-11	2.08E-08	14.74707
TLR2	2.05702	7.192131	7.623896	1.35E-11	7.11E-09	16.05799
MGAM	2.052062	7.754263	6.557685	2.32E-09	4.37E-07	11.12495
AC079305.10	2.046976	5.741511	6.638313	1.59E-09	3.22E-07	11.48913
FOS	2.043344	8.734678	6.979436	3.12E-10	8.24E-08	13.04763
IER3	2.025436	10.94646	6.712946	1.11E-09	2.46E-07	11.82772
CXCL2	2.015147	6.188655	7.602242	1.50E-11	7.69E-09	15.95567
THBD	2.014575	5.609796	9.962034	1.04E-16	6.47E-13	27.35251
ALDH2	2.007903	6.9063	7.248508	8.49E-11	2.97E-08	14.29509
XIST	-2.90841	5.695525	-5.52118	2.60E-07	2.42E-05	6.619292
TSIX	-2.99107	6.834736	-5.53046	2.49E-07	2.35E-05	6.657939

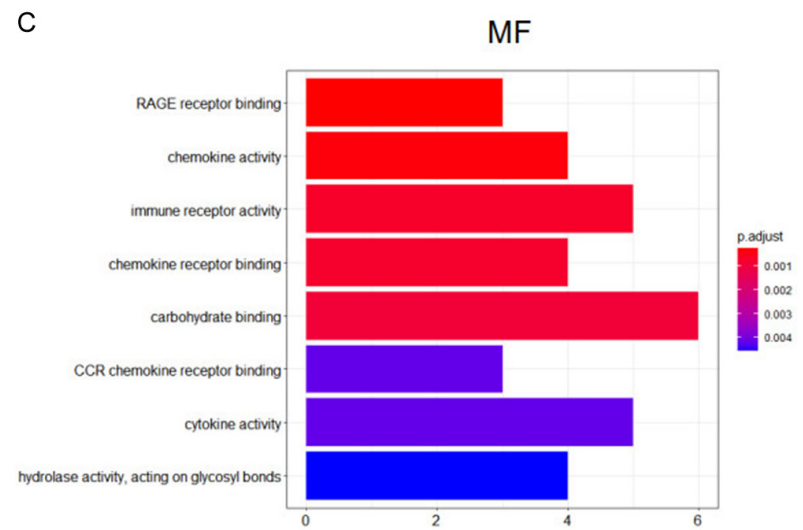
Note: logFC, Log2-Fold Change Between Two Experimental Conditions; AveExpr, Average Expression of Gene Symbol; t, Moderated T-Statistic; p.Value, Raw P-Value; adj.p.Val, P-Value after Adjustment for Multiple Testing; B, B-Statistic or Log-Odds That The Gene Is Differentially Expressed.

ceRNA network in acute myocardial infarction

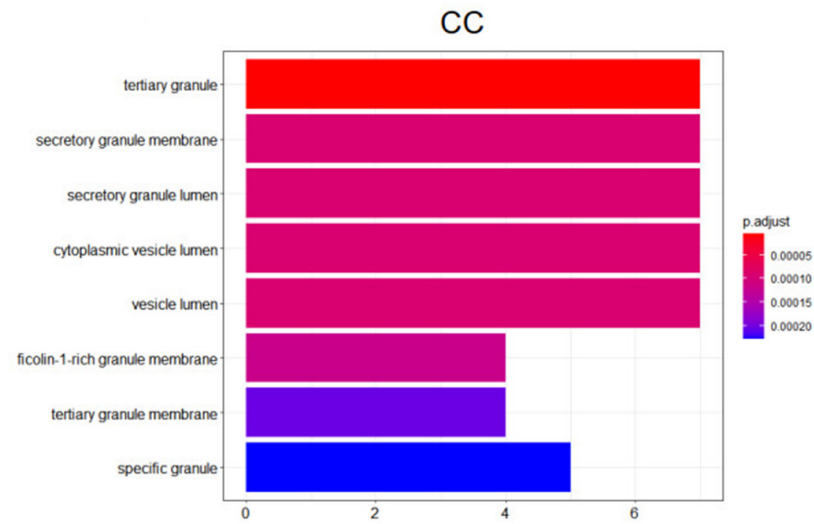
A



C



B



ceRNA network in acute myocardial infarction

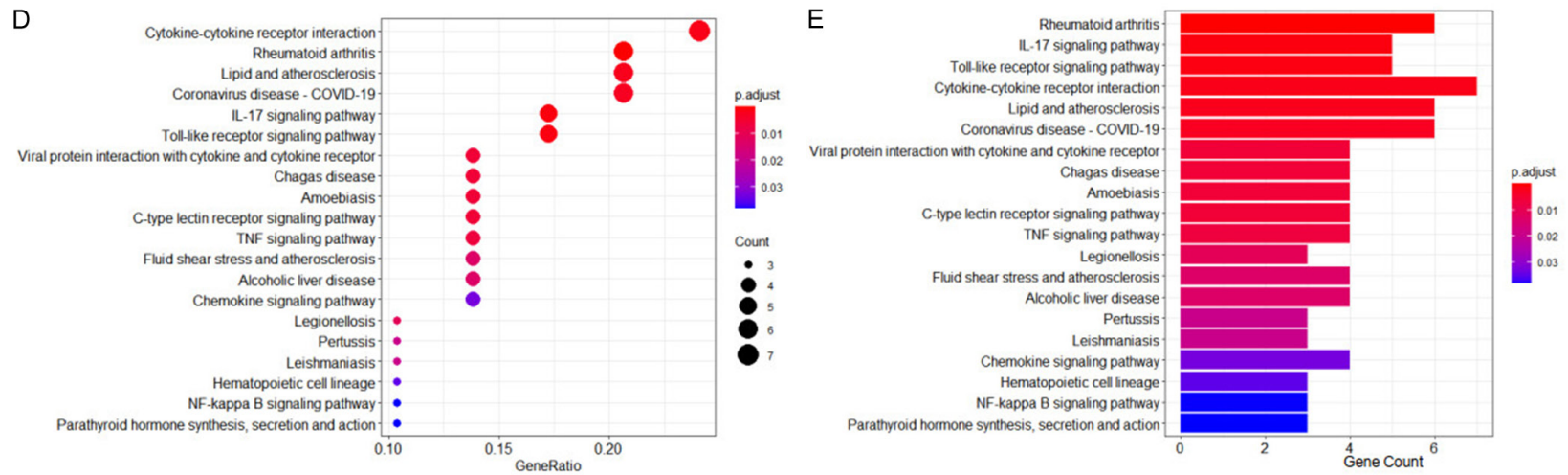


Figure 2. GO function and KEGG enrichment analysis of 46 differentially expressed mRNAs. Barplots of GO enrichment on (A) BP; (B) CC; (C) MF; Bubble chart (D) and barplot (E) of KEGG enrichment of 46 differentially expressed mRNAs. BP, Biological Process, CC, Cellular Component, and MF, Molecular Function.

activity (**Figure 2C**). In addition, the KEGG pathways were also enriched on the immune pathways, such as IL-17 signaling pathway, Toll-like receptor signaling pathway, cytokine-cytokine receptor interaction, TNF signaling pathway, chemokine signaling pathway, and NF-kappaB signaling pathway (**Figure 2D and 2E**).

The PPI network construction and hub genes screening

The PPI network of the 46 differentially expressed genes were analyzed by the STRING online database. As shown in **Figure 3A**, a total of 48 nodes and 165 edges were included in the PPI network. For a better cluster of those genes, we used the MCODE plugin in Cytoscape to produce the network, 18 genes marked with yellow were identified as key genes: C5AR1, AQP9, IL1B, S100A9, CLEC4D, CD83, FCER1G, CXCL2, FCN1, CCL3, CCR5, IL1R2, CSF3, NLRP3, CCL4, FOS, CCL20, and TREM1 (**Figure 3B**). Another plugin of cytoHubba with a higher degree of connectivity hub in Cytoscape was applied to produce the network of the top 10 hub genes. The red color means the higher score of the gene, the top 10 genes were presented as: TLR2, IL1B, CCL4, CCL3, CCR5, TREM1, CXCL2, NLRP3, CSF3, and CCL20 (**Figure 3C**).

Identification of differentially expressed circRNAs and miRNAs

By analyzing GSE160717 dataset based on the criteria of adjusted *P* value < 0.05, a total of 147 differentially expressed circRNAs were identified in **Table 2**, including 74 upregulated circRNAs and 73 downregulated circRNAs. Subsequently, the criteria for screening were set as follows: $|\log_{2}FC| > 2$, and adjusted *P* value < 0.05. Five circRNAs were screened out as follows: circRNA_023461, circRNA_038011, circRNA_400564, circRNA_400027, and circRNA_400101. Meanwhile, GSE24591 dataset based on the criteria of adjusted *P* value < 0.05 showed 65 differentially expressed miRNAs were identified in **Table S1**, 61 miRNAs were downregulated, and four miRNAs were upregulated.

CircRNA-miRNA-mRNA network construction

The starbase database was used for analyzing the downstream of the five circRNAs, 219

downstream targeting miRNAs were identified. To obtain the common same pattern of the predicted targeting miRNAs and differentially expressed miRNAs from GSE24591 dataset, the Venn diagram was applied to the two lists, and six common miRNAs were obtained, including miR-326, miR-590-5p, miR-324-5p, miR-362-3p, miR-199a-5p, and miR-342-3p (**Figure 4A**). Finally, circRNAs, miRNAs and mRNAs with linear connections were used to construct the ceRNA network. Based on the datasets, circRNA_023461 and circRNA_400027 were upregulated, miR-324-5p, miR-326, and miR-590-5p were downregulated, and the four hub genes (CCL20, CCL4, CSF3, and IL1B) were upregulated. CircRNA_023461 (circbank ID: circ_0023461) and circRNA_400027 (circbank ID: circ_0092367) regulated three and two potential miRNA-mRNA axes, respectively. Taken together, the results implied that circRNA_023461 and circRNA_400027 exert important roles in AMI progression.

Discussion

In the present study, we analyzed the circRNA-miRNA-mRNA network based on three datasets, including circRNAs (GSE160717), miRNAs (GSE24591), and mRNAs (GSE66360). The results of the circRNA-miRNA-mRNA network showed that circRNA_023461 and circRNA_400027 regulate five miRNA-mRNA axes, exerting important roles in the pathogenesis of AMI. The hub genes, such as CCL20, CCL4, CSF3, and IL1B, focus on immune response and functions, suggesting the immune modulation play key roles in AMI.

Previous studies have indicated the role of circRNA_023461 in some immune diseases. Zhang et al. identified that circRNA_023461 is downregulated in systemic lupus erythematosus based on GSE84655 dataset, they further predict that circRNA_023461-miR-569-PLAG1, circRNA_023461-miR-569-RSN1, and circRNA_023461-miR-569-NAA30 networks may play important roles in systemic lupus erythematosus [20]. Additionally, Hu et al. found that circRNA_023461 is decreased in Crohn's disease patients' colon biopsies [21]. Notably, Ren et al. revealed that the expression of circ_023461 is upregulated in AMI patients and hypoxia-induced AC16 cells. Downregulation of circ_023461 significantly attenu-

ceRNA network in acute myocardial infarction

Figure 3. The identification of hub genes by PPI network and Cytoscape. A. The PPI network constructed by 46 differentially expressed mRNAs with a linear relationship. B. One module from the PPI network with tight clusters was analyzed using the plugin MCODE in Cytoscape. The hub genes were shown in yellow. C. The top 10 identified hub genes screened by the plugin cytoHubba in Cytoscape are displayed from a high degree value (red) to a low degree value (yellow).

Table 2. The differentially expressed circRNAs in GSE160717 dataset

CircRNA	logFC	AveExpr	t	P.Value	adj.P.Val	B
hsa_circRNA_023461	2.93845	7.692173	5.562576	0.001051	0.048057	-0.33017
hsa_circRNA_038011	2.179865	6.945358	6.230203	0.000554	0.034785	0.32124
hsa_circRNA_400564	2.1508	5.510757	6.371916	0.000487	0.033805	0.451679
hsa_circRNA_400027	2.057797	9.317614	7.363623	0.000209	0.022806	1.294603
hsa_circRNA_400101	2.029329	7.378528	7.08307	0.000263	0.026273	1.067979
hsa_circRNA_001264	1.98056	6.792306	5.475486	0.001147	0.048382	-0.41983
hsa_circRNA_103361	1.97414	10.7009	8.276491	0.000103	0.020653	1.973839
hsa_circRNA_400033	1.973591	10.30548	6.023629	0.000672	0.038111	0.126302
hsa_circRNA_103372	1.886162	10.40032	10.05501	3.13E-05	0.017128	3.079928
hsa_circRNA_001350	1.883575	7.645596	7.559206	0.000179	0.021946	1.447419
hsa_circRNA_001490	1.879577	10.53841	5.946792	0.000723	0.040215	0.052308
hsa_circRNA_404567	1.759295	7.512151	11.04929	1.74E-05	0.017064	3.595952
hsa_circRNA_003997	1.758564	8.356	9.379864	4.81E-05	0.017128	2.690218
hsa_circRNA_104310	1.738267	10.1806	8.323402	0.0001	0.020653	2.006502
hsa_circRNA_000781	1.708975	8.277767	6.737856	0.000352	0.027551	0.776565
hsa_circRNA_092523	1.682398	9.273217	7.748058	0.000154	0.020653	1.591092
hsa_circRNA_066869	1.675352	6.766885	6.852718	0.000319	0.027448	0.875109
hsa_circRNA_075549	1.610102	7.483581	7.504592	0.000187	0.022008	1.405165
hsa_circRNA_101522	1.599071	9.583808	5.402357	0.001236	0.049566	-0.49599
hsa_circRNA_404807	1.586236	8.199631	9.121444	5.72E-05	0.018594	2.531733
hsa_circRNA_103758	-1.52398	5.900806	-6.21106	0.000564	0.035032	0.303415
hsa_circRNA_406422	-1.54965	7.175526	-6.71885	0.000358	0.027551	0.760108
hsa_circRNA_103123	-1.57804	6.377317	-9.79975	3.67E-05	0.017128	2.936576
hsa_circRNA_103111	-1.5909	6.083552	-9.52537	4.38E-05	0.017128	2.777119
hsa_circRNA_015677	-1.59201	5.269776	-13.8913	4.07E-06	0.017064	4.767536
hsa_circRNA_103110	-1.67391	6.82673	-8.23276	0.000107	0.020653	1.943205
hsa_circRNA_103560	-1.70771	6.842923	-8.88957	6.69E-05	0.018594	2.384854
hsa_circRNA_068655	-1.84045	6.465976	-8.32547	9.99E-05	0.020653	2.007936

Note: logFC, Log2-Fold Change Between Two Experimental Conditions; AveExpr, Average Expression of Gene Symbol; t, Moderated T-Statistic; p.Value, Raw P-Value; adj.p.Val, P-Value after Adjustment for Multiple Testing; B, B-Statistic or Log-Odds That The Gene Is Differentially Expressed.

ates hypoxia-induced dysfunction in AC16 cells through elevating the level of miR-370-3p and inhibiting the expression of PDE4D [22]. And Wu et al. also found the expression of circ_023461 was increased in AC16 cell hypoxia model, suggesting the potential role of circ_023461 in the progression of AMI [23]. For circ_400027, Yu et al. uncovered that circ_400027 is significantly decreased in pancreatic cancer tissues and cell lines, and high circ_400027 expression is associated with

improved survival time in patients with pancreatic cancer. They further revealed that circ_400027 suppresses epithelial-mesenchymal transition (EMT) and gemcitabine resistance in pancreatic cancer cells by downregulating the level of miR-1206 and enhancing the expression of ESRP1 [24]. Compared with these studies, our study found that circRNA_023461 and circRNA_400027 were downregulated in AMI tissues, which are the same with Ren's group, and the downstream of these two circRNAs

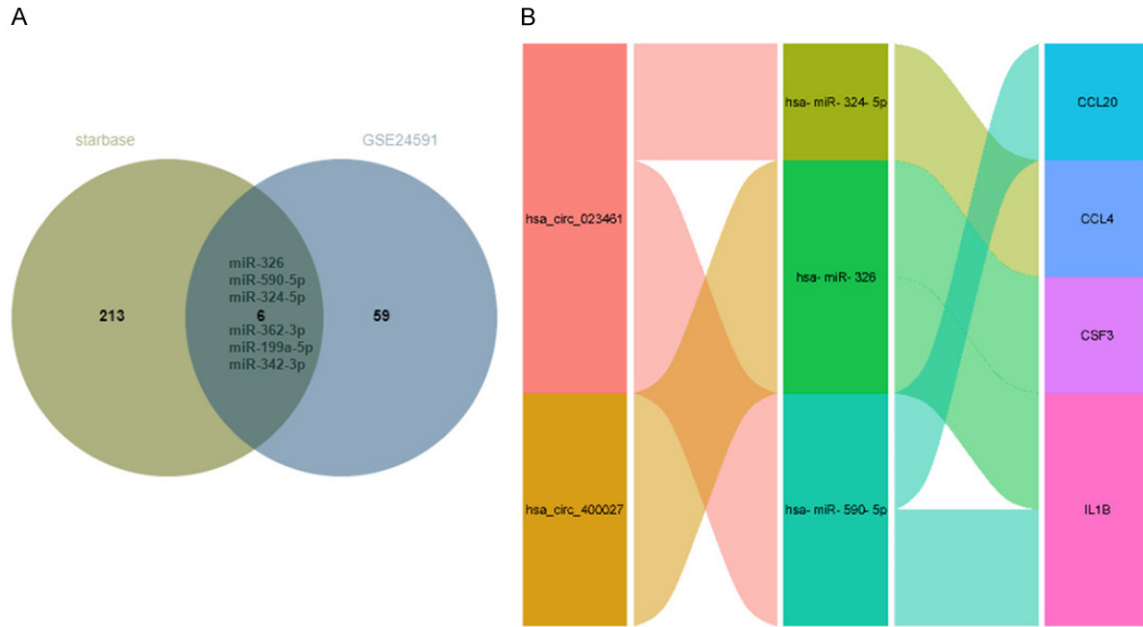


Figure 4. The circRNA-miRNA-mRNA network. A. A Venn diagram of miRNAs prediction of the five circRNAs from the starbase database and the differentially expressed miRNAs from GSE24591. B. The ceRNA interaction network of circRNA-miRNA-mRNA. The first column represents circRNAs, the second column represents miRNAs, and the third column represents mRNAs. Connection represents interaction.

were miR-326, miR-590-5p, and miR-324-5p by interacting with the GSE24591 miRNA dataset. Therefore, circRNA_023461 and circRNA_400027 may participate in the progression of AMI.

Not surprisingly, miR-326, miR-590-5p, and miR-324-5p have been involved in the development of various cancers. For instance, Wei et al. reported that miR-326 expression is decreased in bladder cancer, and is sponged by circ_0139402 to upregulate PAX8 expression, facilitating cell proliferation, migration, invasion, and EMT [25]. Wang et al. indicated that circ_0020123 accelerates cell proliferation and migration in non-small cell lung cancer progression by inhibiting miR-590-5p to enhance the level of THBS2 [26]. Li et al. demonstrated that miR-324-5p is repressed in glioblastoma, and circRNA SERPINE2 facilitates glioblastoma cell proliferation and colony formation by inhibiting miR-324-5p to increase BCL2 expression [27]. As regard to MI, miR-326-5p significantly promotes the angiogenic capacity of endothelial progenitor cells, and transplantation of miR-326-5p-overexpressing endothelial progenitor cells could improve cardiac function for AMI therapy [28]. In addition, miR-590-5p

represses cardiosphere-derived stem cells differentiation via downregulation of TGFB signaling, such as the reduction of TGFBR2 expression [29]. Shao also demonstrated that miR-590-5p involved in lncRNA ACSL4-miR590-5p-IL1B axis could be used as RNA regulatory pathways affecting AMI disease progression [30]. Sun et al. revealed that TUG1 knockdown via enhancing miR-590 expression to suppress cardiac fibrosis after AMI in cardiac fibroblasts [31]. Administration of miR-590-3p immediately after myocardial infarction in mice resulted in marked reduction of infarct size and persistent recovery of cardiac function [32]. Another work also reported that rapid delivery of miR-590-3p using targeted exosomes could treat AMI by promoting myocardial proliferation [33]. Recently, Ji's group found that miR-324-5p-modified adipose-derived stem cells evidently improves post-MI myocardial repair by targeting Toll-interacting protein in myocardial tissues [34]. Huang et al. elucidated that silence of lncRNA Gpr19 repressed IR injury after AMI by inhibiting apoptosis and oxidative stress via upregulating miR-324-5p and downregulating Mtrf1 expression [35]. Wang et al. revealed that miR-324-5p inhibited mitochondrial fission, cardiomyocyte apoptosis and MI by down-

regulating Mtrf1 translation [36]. These researches provide prospective insight into the therapeutic role of these miRNAs in AMI. Consistent with previous studies, our findings also suggested that miR-326, miR-590-5p, and miR-324-5p involving in the ceRNA network may affect the progression of AMI, which could be effective targets for the treatment of AMI.

CCL genes belong to the subfamily of small cytokine CC genes. Cytokines are a family of secreted proteins involved in immunoregulatory and inflammatory processes. Recently, Zhou et al. found that increased mRNA levels of macrophage/microglia activation marker Iba1, chemokine ligands (CXCL10, CCL20), chemokine receptor CCR5 and pro-inflammatory cytokine IL6 in the left stellate ganglion in the model of 4-week MI beagles [37]. Safa et al. identified that CCL20 level in the serum is significantly increased in patients with ischemic heart disease [38]. Nagasaka et al. demonstrated that TDAG8 negatively regulates the transcription of the chemokine CCL20 and inhibits the number of infiltrating IL-17A-producing $\gamma\delta$ T cells that express CCR6, a receptor for CCL20, presenting a cardioprotective effects against MI [39]. Furthermore, Yao et al. gave an important bioinformatics analysis predicting that three-gene signature consisting of CCL20, IL1R2, and ITLN1 could effectively distinguish patients with MI [40]. And Zhang et al. found that down-regulated expression of CCL4 correlating with immune response was found in AMI patients [41]. CSF3 encodes a member of the IL-6 superfamily of cytokines, which controls the production, differentiation, and function of granulocytes, a type of white blood cell that are part of the innate immune response. Recently, Wang et al. analyzed the gene expression profile of peripheral blood monocytes in different stages of coronary artery disease by transcriptome sequencing, the results showed that immune response related CSF3, IL-1A, CCR7, and IL-18 are significantly upregulated in the patients' peripheral blood monocytes [42]. IL-1B is also a key pro-inflammatory cytokine that has been associated with the development of MI. Pan et al. reported that IL1B rs1143634 C/T polymorphism associates with the risk and blood lipid levels of MI in an Eastern Chinese Han population [43]. Chen et al. also analyzed key genes in AMI based on three GEO datasets (GSE775, GSE19322, and GSE97494), the

results showed that 18 key genes, including IL-1B, CXCL5, ARG1, CXCL1, SPP1, SELP, PTX3, TNFAIP6, MMP8, SERPINE1, PTGS2, IL6, ILLR2, CCL3, CCR1, HMOX1, CXCL2, and CCL2. CCR1 was the most fundamental gene in PPI network [44]. Our study also found related key genes in AMI, such as IL-1B, CXCL2, and CCL3. Recently, Zhang et al. demonstrated that IL1B is a target in the lncRNA-miRNA-mRNA axis in the pathogenesis of ischemic stroke. They found that lncRNA MIAT and IL1B are increased and miR-874-3p is decreased in ischemic stroke patients, lncRNA MIAT impairs neurological function by elevating miR-874-3p-targeted IL1B [45]. And Wu et al. reported that IL1B was considered as a diagnostic marker for AMI. The immune cell infiltration analysis indicated that IL1B were correlated with neutrophils, monocytes, resting natural killer (NK) cells, gamma delta T cells, and CD4 memory resting T cells. The fractions of monocytes and neutrophils were significantly higher in AMI tissues than in control tissues [46]. Notably, our results found the different expression genes in AMI were enriched in neutrophil chemotaxis, neutrophil migration, granulocyte chemotaxis, granulocyte migration, neutrophil degranulation, myeloid leukocyte migration, and neutrophil activation, implying the immune functions play crucial roles in the progression of AMI. Moreover, some immune pathways, such as IL-17 signaling pathway, Toll-like receptor signaling pathway, cytokine-cytokine receptor interaction, TNF signaling pathway, chemokine signaling pathway, and NF-kappaB signaling pathway were enriched in AMI patients, suggesting the immune response pathways participate in the development of AMI. Consistently, Liu et al. identified important genes related to ferroptosis and hypoxia in AMI based on Weighted Gene Co-Expression Network Analysis (WGCNA) of the GSE4648 data. The key genes were mainly related to ERK1 and ERK2 cascade, TNF signaling pathway, and MAPK signaling pathway [47]. Li et al. found that elevated levels of proinflammatory cytokines, toll-like receptors, and TNF- α pathway were associated with recurrent MI after coronary stenting [48]. Additionally, upregulation of NF-kappaB signaling pathway significantly aggravated the development of AMI [49-51]. Considering the key roles and signaling pathways of these immune-related genes in cardiovascular diseases, especially

AMI, they may be prospective therapeutic targets of AMI.

Some limitations still exist in our study. The number of the clinical samples in the datasets is small, further samples need to be investigated to verify our results. Furthermore, *in vitro* and *in vivo* experiments should be determined to confirm the biological role of these circRNA-miRNA-mRNA axes.

Conclusion

In summary, this study uncovered the circRNA-miRNA-mRNA network based on three AMI datasets. The differentially expressed genes, including CCL20, CCL4, CSF3, and IL1B, focus on immune response and functions. And many immune response pathways participate in the development of AMI, such as IL-17 signaling pathway, Toll-like receptor signaling pathway, cytokine-cytokine receptor interaction, TNF signaling pathway, chemokine signaling pathway, and NF-kappaB signaling pathway. Furthermore, circRNA_023461 and circRNA_400027 regulate five miRNA-mRNA axes, exerting important roles in AMI progression. Our findings may provide new insights into AMI and improve the diagnose and therapeutic strategies for AMI patients.

Acknowledgements

We acknowledge GEO database for providing their platforms and contributors for uploading their meaningful datasets. GEO belong to public databases. The patients involved in the database have obtained ethical approval. Users can download relevant data for free for research and publish relevant articles.

Disclosure of conflict of interest

None.

Address correspondence to: Hui Liu, Department of Cardiovascular Surgery, Linfen Central Hospital, No. 17, Jiefang Western Road, Linfen 041000, Shanxi, China. Tel: +86-15034348188; E-mail: liuhuidocor@163.com

References

[1] Anderson JL and Morrow DA. Acute myocardial infarction. *N Engl J Med* 2017; 376: 2053-2064.

[2] Roger VL, Go AS, Lloyd-Jones DM, Benjamin EJ, Berry JD, Borden WB, Bravata DM, Dai S, Ford ES, Fox CS, Fullerton HJ, Gillespie C, Hailpern SM, Heit JA, Howard VJ, Kissela BM, Kittner SJ, Lackland DT, Lichtman JH, Lisabeth LD, Makuc DM, Marcus GM, Marelli A, Matchar DB, Moy CS, Mozaffarian D, Mussolino ME, Nichol G, Paynter NP, Soliman EZ, Sorlie PD, Sotodehnia N, Turan TN, Virani SS, Wong ND, Woo D and Turner MB; American Heart Association Statistics Committee and Stroke Statistics Subcommittee. Executive summary: heart disease and stroke statistics-2012 update: a report from the American Heart Association. *Circulation* 2012; 125: 188-197.

[3] Sulo G, Iglund J, Sulo E, Øverland S, Egeland GM, Vollset SE and Tell GS. Mortality following first-time hospitalization with acute myocardial infarction in Norway, 2001-2014: time trends, underlying causes and place of death. *Int J Cardiol* 2019; 294: 6-12.

[4] Hajar R. Evolution of myocardial infarction and its biomarkers: a historical perspective. *Heart Views* 2016; 17: 167-172.

[5] Zhang F, Zhang R, Zhang X, Wu Y, Li X, Zhang S, Hou W, Ding Y, Tian J, Sun L and Kong X. Comprehensive analysis of circRNA expression pattern and circRNA-miRNA-mRNA network in the pathogenesis of atherosclerosis in rabbits. *Ageing (Albany NY)* 2018; 10: 2266-2283.

[6] Baek D, Villen J, Shin C, Camargo FD, Gygi SP and Bartel DP. The impact of microRNAs on protein output. *Nature* 2008; 455: 64-71.

[7] Laressergues D, Couzigou JM, Clemente HS, Martinez Y, Dunand C, Becard G and Combier JP. Primary transcripts of microRNAs encode regulatory peptides. *Nature* 2015; 520: 90-93.

[8] Zhai X, Zhang Y, Xin S, Cao P and Lu J. Insights into the involvement of circular RNAs in autoimmune diseases. *Front Immunol* 2021; 12: 622316.

[9] Shi Y, Jia X and Xu J. The new function of circRNA: translation. *Clin Transl Oncol* 2020; 22: 2162-2169.

[10] Hansen TB, Jensen TI, Clausen BH, Bramsen JB, Finsen B, Damgaard CK and Kjems J. Natural RNA circles function as efficient microRNA sponges. *Nature* 2013; 495: 384-388.

[11] Zhang J, Luo CJ, Xiong XQ, Li J, Tang SH, Sun L and Su Q. MiR-21-5p-expressing bone marrow mesenchymal stem cells alleviate myocardial ischemia/reperfusion injury by regulating the circRNA_0031672/miR-21-5p/programmed cell death protein 4 pathway. *J Geriatr Cardiol* 2021; 18: 1029-1043.

[12] Song H, Yang Y, Sun Y, Wei G, Zheng H, Chen Y, Cai D, Li C, Ma Y, Lin Z, Shi X, Liao W, Liao Y, Zhong L and Bin J. Circular RNA Cdy1 promotes abdominal aortic aneurysm formation by in-

ceRNA network in acute myocardial infarction

- ducing M1 macrophage polarization and M1-type inflammation. *Mol Ther* 2022; 30: 915-931.
- [13] Huang JG, Tang X, Wang JJ, Liu J, Chen P and Sun Y. A circular RNA, circUSP36, accelerates endothelial cell dysfunction in atherosclerosis by adsorbing miR-637 to enhance WNT4 expression. *Bioengineered* 2021; 12: 6759-6770.
- [14] Zhang L, Han B, Liu H, Wang J, Feng X, Sun W, Cai D, Jia H and Jiang D. Circular RNA circACSL1 aggravated myocardial inflammation and myocardial injury by sponging miR-8055 and regulating MAPK14 expression. *Cell Death Dis* 2021; 12: 487.
- [15] Wang S, Li L, Deng W and Jiang M. CircRNA MFACR is upregulated in myocardial infarction and downregulates miR-125b to promote cardiomyocyte apoptosis induced by hypoxia. *J Cardiovasc Pharmacol* 2021; 78: 802-808.
- [16] Liu X, Wang M, Li Q, Liu W, Song Q and Jiang H. CircRNA ACAP2 induces myocardial apoptosis after myocardial infarction by sponging miR-29. *Minerva Med* 2022; 113: 128-134.
- [17] Zhu Y, Zhao P, Sun L, Lu Y, Zhu W, Zhang J, Xiang C, Mao Y, Chen Q and Zhang F. Overexpression of circRNA SNRK targets miR-103-3p to reduce apoptosis and promote cardiac repair through GSK3beta/beta-catenin pathway in rats with myocardial infarction. *Cell Death Discov* 2021; 7: 84.
- [18] Mao J, Zhou Y, Lu L, Zhang P, Ren R, Wang Y and Wang J. Identifying a serum exosomal-associated lncRNA/circRNA-miRNA-mRNA network in coronary heart disease. *Cardiol Res Pract* 2021; 2021: 6682183.
- [19] Liu Y, Liu N and Liu Q. Constructing a ceRNA-immunoregulatory network associated with the development and prognosis of human atherosclerosis through weighted gene co-expression network analysis. *Aging (Albany NY)* 2021; 13: 3080-3100.
- [20] Zhang J, Liu Y and Shi G. The circRNA-miRNA-mRNA regulatory network in systemic lupus erythematosus. *Clin Rheumatol* 2021; 40: 331-339.
- [21] Hu YA, Zhu Y, Liu G, Yao X, Yan X, Yang Y, Wang W, Zou X and Li X. Expression profiles of circular RNAs in colon biopsies from Crohn's disease patients by microarray analysis. *J Clin Lab Anal* 2021; 35: e23788.
- [22] Ren K, Li B, Jiang L, Liu Z, Wu F, Zhang Y, Liu J and Duan W. Circ_0023461 silencing protects cardiomyocytes from hypoxia-induced dysfunction through targeting miR-370-3p/PDE4D signaling. *Oxid Med Cell Longev* 2021; 2021: 8379962.
- [23] Wu J, Li C, Lei Z, Cai H, Hu Y, Zhu Y, Zhang T, Zhu H, Cao J and Hu X. Comprehensive analysis of circRNA-miRNA-mRNA regulatory network and novel potential biomarkers in acute myocardial infarction. *Front Cardiovasc Med* 2022; 9: 850991.
- [24] Yu S, Wang M, Zhang H, Guo X and Qin R. Circ_0092367 inhibits EMT and gemcitabine resistance in pancreatic cancer via regulating the miR-1206/ESRP1 axis. *Genes (Basel)* 2021; 12: 1701.
- [25] Wei B, Wang Z, Lian Q, Chi B and Ma S. Hsa_circ_0139402 promotes bladder cancer progression by regulating hsa-miR-326/PAX8 signaling. *Dis Markers* 2022; 2022: 9899548.
- [26] Wang L, Zhao L and Wang Y. Circular RNA circ_0020123 promotes non-small cell lung cancer progression by sponging miR-590-5p to regulate THBS2. *Cancer Cell Int* 2020; 20: 387.
- [27] Li D, Li L, Chen X, Yang W and Cao Y. Circular RNA SERPINE2 promotes development of glioblastoma by regulating the miR-361-3p/miR-324-5p/BCL2 signaling pathway. *Mol Ther Oncolytics* 2021; 22: 483-494.
- [28] Li X, Xue X, Sun Y, Chen L, Zhao T, Yang W, Chen Y and Zhang Z. MicroRNA-326-5p enhances therapeutic potential of endothelial progenitor cells for myocardial infarction. *Stem Cell Res Ther* 2019; 10: 323.
- [29] Ekhteraei-Tousi S, Mohammad-Soltani B, Sa-deghizadeh M, Mowla SJ, Parsi S and Soleimani M. Inhibitory effect of hsa-miR-590-5p on cardiosphere-derived stem cells differentiation through downregulation of TGFB signaling. *J Cell Biochem* 2015; 116: 179-191.
- [30] Shao G. Integrated RNA gene expression analysis identified potential immune-related biomarkers and RNA regulatory pathways of acute myocardial infarction. *PLoS One* 2022; 17: e0264362.
- [31] Sun Q, Luo M, Gao Z, Han X, Yan Z, Xie S, Zhao H and Sun H. TUG1 knockdown suppresses cardiac fibrosis after myocardial infarction. *Mamm Genome* 2021; 32: 435-442.
- [32] Lesizza P, Prosdocimo G, Martinelli V, Sinagra G, Zacchigna S and Giacca M. Single-dose intracardiac injection of pro-regenerative MicroRNAs improves cardiac function after myocardial infarction. *Circ Res* 2017; 120: 1298-1304.
- [33] Wang Y, Ding N, Guan G, Liu G, Huo D, Li Y, Wei K, Yang J, Cheng P and Zhu C. Rapid delivery of hsa-miR-590-3p using targeted exosomes to treat acute myocardial infarction through regulation of the cell cycle. *J Biomed Nanotechnol* 2018; 14: 968-977.
- [34] Ji Z, Wang C and Tong Q. Role of miRNA-324-5p-modified adipose-derived stem cells in post-myocardial infarction repair. *Int J Stem Cells* 2021; 14: 298-309.

ceRNA network in acute myocardial infarction

- [35] Huang L, Guo B, Liu S, Miao C and Li Y. Inhibition of the lncRNA Gpr19 attenuates ischemia-reperfusion injury after acute myocardial infarction by inhibiting apoptosis and oxidative stress via the miR-324-5p/Mtfr1 axis. *IUBMB Life* 2020; 72: 373-383.
- [36] Wang K, Zhang DL, Long B, An T, Zhang J, Zhou LY, Liu CY and Li PF. NFAT4-dependent miR-324-5p regulates mitochondrial morphology and cardiomyocyte cell death by targeting Mtfr1. *Cell Death Dis* 2015; 6: e2007.
- [37] Zhou Z, Liu C, Xu S, Wang J, Guo F, Duan S, Deng Q, Sun J, Yu F, Zhou Y, Wang M, Wang Y, Zhou L, Jiang H and Yu L. Metabolism regulator adiponectin prevents cardiac remodeling and ventricular arrhythmias via sympathetic modulation in a myocardial infarction model. *Basic Res Cardiol* 2022; 117: 34.
- [38] Safa A, Rashidinejad HR, Khalili M, Dabiri S, Nemati M, Mohammadi MM and Jafarzadeh A. Higher circulating levels of chemokines CXCL10, CCL20 and CCL22 in patients with ischemic heart disease. *Cytokine* 2016; 83: 147-157.
- [39] Nagasaka A, Mogi C, Ono H, Nishi T, Horii Y, Ohba Y, Sato K, Nakaya M, Okajima F and Kurose H. The proton-sensing G protein-coupled receptor T-cell death-associated gene 8 (TD-AG8) shows cardioprotective effects against myocardial infarction. *Sci Rep* 2017; 7: 7812.
- [40] Yao Y, Zhao J, Zhou X, Hu J and Wang Y. Potential role of a three-gene signature in predicting diagnosis in patients with myocardial infarction. *Bioengineered* 2021; 12: 2734-2749.
- [41] Zhang S, Liu W, Liu X, Qi J and Deng C. Biomarkers identification for acute myocardial infarction detection via weighted gene co-expression network analysis. *Medicine (Baltimore)* 2017; 96: e8375.
- [42] Wang C, Song C, Liu Q, Zhang R, Fu R, Wang H, Yin D, Song W, Zhang H and Dou K. Gene expression analysis suggests immunological changes of peripheral blood monocytes in the progression of patients with coronary artery disease. *Front Genet* 2021; 12: 641117.
- [43] Pan Q, Hui D and Hu C. A variant of IL1B is associated with the risk and blood lipid levels of myocardial infarction in eastern Chinese individuals. *Immunol Invest* 2022; 51: 1162-1169.
- [44] Chen DQ, Kong XS, Shen XB, Huang MZ, Zheng JP, Sun J and Xu SH. Identification of differentially expressed genes and signaling pathways in acute myocardial infarction based on integrated bioinformatics analysis. *Cardiovasc Ther* 2019; 2019: 8490707.
- [45] Zhang S, Zhang Y, Wang N, Wang Y, Nie H, Zhang Y, Han H, Wang S, Liu W and Bo C. Long non-coding RNA MIAT impairs neurological function in ischemic stroke via up-regulating microRNA-874-3p-targeted IL1B. *Brain Res Bull* 2021; 175: 81-89.
- [46] Wu Y, Jiang T, Hua J, Xiong Z, Chen H, Li L, Peng J and Xiong W. Integrated bioinformatics-based analysis of hub genes and the mechanism of immune infiltration associated with acute myocardial infarction. *Front Cardiovasc Med* 2022; 9: 831605.
- [47] Liu K, Chen S and Lu R. Identification of important genes related to ferroptosis and hypoxia in acute myocardial infarction based on WGCNA. *Bioengineered* 2021; 12: 7950-7963.
- [48] Li X, Guo D, Chen Y and Hu Y. Toll-like receptors/TNF-alpha pathway crosstalk and impact on different sites of recurrent myocardial infarction in elderly patients. *Biomed Res Int* 2022; 2022: 1280350.
- [49] Wang X, Su J, Lin Z, Liu K and Zhuang Y. PINCH1 knockout aggravates myocardial infarction in mice via mediating the NF-kappaB signaling pathway. *Exp Ther Med* 2022; 23: 62.
- [50] Ning H, Chen H, Deng J, Xiao C, Xu M, Shan L, Yang C and Zhang Z. Exosomes secreted by FNDC5-BMMSCs protect myocardial infarction by anti-inflammation and macrophage polarization via NF-kappaB signaling pathway and Nrf2/HO-1 axis. *Stem Cell Res Ther* 2021; 12: 519.
- [51] Shi H, Zhou P, Gao G, Liu PP, Wang SS, Song R, Zou YY, Yin G and Wang L. Astragaloside IV prevents acute myocardial infarction by inhibiting the TLR4/MyD88/NF-kappaB signaling pathway. *J Food Biochem* 2021; 45: e13757.

ceRNA network in acute myocardial infarction

Table S1. The differentially expressed miRNAs in GSE24591 dataset

ID	log2 (fold change)	-log10 (adj.P.Val)
hsa-miR-34a	1.096351936	3.261490311
hsa-miR-30a	0.895789115	2.884104259
hsa-miR-342-3p	0.783525428	2.87957515
hsa-miR-432	0.660890791	1.95747434
hsa-miR-454	-0.429150498	1.961490968
hsa-miR-324-5p	-0.437145862	2.065633878
hsa-miR-126	-0.472458178	1.975821171
hsa-miR-18b	-0.484177986	1.940577686
hsa-miR-148b	-0.484385132	2.164269352
hsa-miR-106b	-0.49516748	2.180678228
hsa-miR-627	-0.500350924	2.006040082
hsa-miR-200a	-0.511576894	2.380123759
hsa-miR-27a	-0.51804506	2.155417652
hsa-miR-140-5p	-0.536912582	2.364772368
hsa-miR-199b-3p	-0.551858404	2.207260607
hsa-miR-146b-5p	-0.556687171	2.144779571
hsa-miR-15b	-0.564301756	1.941404487
hsa-miR-326	-0.574824158	2.471520985
hsa-miR-628-5p	-0.584201713	2.050046037
hsa-miR-148a	-0.608444257	2.377815127
hsa-miR-30e	-0.611992995	2.776395273
hsa-miR-199a-5p	-0.636618962	2.849330593
hsa-miR-20a	-0.659248665	2.706333752
hsa-miR-660	-0.681856846	2.582050004
hsa-miR-21	-0.682735824	2.826781217
hsa-miR-141	-0.688953783	2.480373954
hsa-miR-26b	-0.731643052	2.849842583
hsa-miR-30d	-0.731947928	2.700268837
hsa-miR-7	-0.752226074	2.205541393
hsa-miR-625	-0.760772894	2.094597009
hsa-miR-15a	-0.76411857	2.734428419
hsa-miR-192	-0.765060539	2.480118886
hsa-miR-19b	-0.786968068	2.704252027
hsa-miR-142-5p	-0.813378145	3.031197706
hsa-miR-335	-0.813929876	2.701125872
hsa-miR-29c	-0.817439947	3.038769978
hsa-miR-7-1	-0.825556659	2.558296573
hsa-miR-215	-0.832049846	2.680424473
hsa-miR-374a	-0.844568963	2.64726473
hsa-miR-548c-5p	-0.862953656	2.282130147
hsa-miR-624	-0.894550888	2.527080088
hsa-miR-301a	-0.909976459	3.184287755
hsa-miR-340	-0.955041963	3.092686993
hsa-miR-139-3p	-1.011280172	2.620827572
hsa-miR-150	-1.014509817	2.802553829
hsa-miR-17	-1.040488246	3.686802378
hsa-miR-548a-5p	-1.045410073	3.945618804

ceRNA network in acute myocardial infarction

hsa-miR-19a	-1.063831783	3.182283162
hsa-miR-24-1	-1.06975106	3.495521749
hsa-miR-142-3p	-1.079085274	3.589527498
hsa-miR-598	-1.140742727	3.550844817
hsa-miR-33b	-1.16806474	3.673421355
hsa-miR-9	-1.184708206	2.699705831
hsa-miR-101	-1.190077885	3.614319293
hsa-miR-590-5p	-1.19770241	3.515807167
hsa-miR-136	-1.260201969	1.963606874
hsa-let-7d*	-1.329952296	2.563970344
hsa-miR-33a	-1.33940043	3.69937145
hsa-miR-768-5p	-1.341879691	2.25859658
hsa-miR-219-5p	-1.342817633	4.286107867
hsa-miR-29b	-1.459020883	3.996988195
hsa-miR-545	-1.504666212	4.43577796
hsa-miR-362-3p	-1.507771538	3.553533109
hsa-miR-32	-1.716461507	4.516791844
hsa-miR-1	-1.730783608	2.094301607

Note: log₂ (fold change), Log₂-Fold Change Between Two Experimental Conditions; -log₁₀ (adj.P.Val), Log₁₀-Fold Change of P-Value after Adjustment For Multiple Testing.